Superresolution by localization of quantum dots using blinking statistics

Keith A. Lidke[1], **Bernd Rieger**[1], **Thomas M. Jovin**[1] **and Rainer Heintzmann**[1,2]

[1] *Department of Molecular Biology, Max Planck Institute for Biophysical Chemistry, Am Fassberg 11, 37077 Göttingen, Germany*

klidke@gwdg.de

[2] *King's College London, Randall Division of Cell and Molecular Biophysics, New Hunt's House, Guy's Campus, London SE1 1UL*

rainer.heintzmann@kcl.ac.uk

Abstract: In microscopy, single fluorescence point sources can be localized with a precision several times greater than the resolution limit of the microscope. We show that the intermittent fluorescence or 'blinking' of quantum dots can analyzed by an Independent Component Analysis so as to identify the light emitted by each individual nanoparticle, localize it precisely, and thereby resolve groups of closely spaced ($< \lambda/30$) quantum dots. Both simulated and experimental data demonstrate that this technique is superior to localization based on Maximum Likelihood Estimation of the sum image under the assumption of point emitters. This technique has general application to any emitter with non-Gaussian temporal intensity distribution, including triplet state blinking. When applied to the labeling of structures, a high resolution "image" consisting of individually localized points may be reconstructed leading to the term "Pointillism".

OCIS codes: (100.6640) Superresolution; (180.2520) Fluorescence microscopy; (100.3020) Image reconstruction–restoration; (100.5010) Pattern Recognition; (350.5730) Resolution

References and links

1. H. Grecco, K.A. Lidke, R. Heintzmann, D.S. Lidke, C. Spagnuolo, O.E. Martinez, E.A. Jares-Erijman, and T.M. Jovin. "Ensemble and single particle photophysical properties (two-photon excitation, anisotropy, FRET, lifetime, spectral conversion) of commercial quantum dots in solution and in live cells," Microsc. Res. Tech. **65**, 169–179 (2004).
2. X. Michalet, F. F. Pinaud, L. A. Bentolila, J. M. Tsay, S. Doose, J. J. Li, G. Sundaresan, A. M. Wu, S. S. Gambhir, and S. Weiss. "Quantum dots for live cells, in vivo imaging, and diagnostics," Science **307**, 538–544 (2005).
3. D.S. Lidke, P. Nagy, R. Heintzmann, D.J. Arndt-Jovin, J.N. Post, H. Grecco, E.A. Jares-Erijman, and T.M. Jovin. "Quantum dot ligands provide new insights into erbB/HER receptor-mediated signal transduction," Nat. Biotechnol. **22**, 198–203 (2004).
4. M.G.L. Gustafsson, D.A. Agard, and J.W. Sedat. "I^5M-3D widefield light microscopy with better than 100 nm axial resolution," J. Microsc. **195**, 10–16 (1999).
5. S.W. Hell, S. Lindek, C. Cremer, and E.H.K. Stelzer. "Measurement of the 4pi-confocal point spread function proves 75 nm axial resolution," Appl. Phys. Lett. **64**, 1335–1337 (1994).
6. S.W. Hell and J. Wichmann. "Breaking the diffraction limit resolution by stimulated emission: stimulated-emission-depletion microscopy," Opt. Lett. **19**, 780–783 (1994).
7. T.A. Klar, M. Dyba, and S.W. Hell. "Stimulated emission depletion microscopy with an offset depleting beam," Appl. Phys. Lett. **78**, 393–395 (2001).
8. R. Heintzmann, T.M. Jovin, and C. Cremer. "Saturated patterned excitation microscopy – a concept for optical resolution improvement," J. Opt. Soc. Am. A **19**, 1599–1609 (2002).

#7770 - $15.00 USD Received 10 June 2005; revised 14 August 2005; accepted 26 August 2005

9. R.J. Ober, S. Ram, and S.E. Ward. "Localization accuracy in single-molecule microscopy," Biophys. J. **86**, 1185–1200 (2004).
10. A. Yildiz, J.N. Forkey, S.A. McKinney, T. Ha, Y.E. Goldman, and P.R. Selvin. "Myosin V walks hand-over-hand: Single fluorophore imaging with 1.5 nm localization," Science **300**, 2061–2066 (2003).
11. A. Esa, P. Edelmann, G. Kreth, L. Trakhtenbrot, N. Amariglio, G. Rechavi, M. Hausmann, and C. Cremer. "Three-dimensional spectral precision distance microscopy of chromatin nanostructures after triple-colour DNA labelling: a study of the BCR region on chromosome 22 and the Philadelphia chromosome," J. Microsc. **199**, 96–105 (2000).
12. M. Heilemann, D.P. Herten, R. Heintzmann, C. Cremer, C. Müller, P. Tinnefeld, K.D. Weston, J. Wolfrum, and M. Sauer. "High-resolution colocalization of single dye molecules by fluorescence lifetime imaging microscopy," Anal. Chem. **74**, 3511–3517 (2002).
13. M.P. Gordon, T. Ha, and P.R. Selvin. "Single-molecule high-resolution imaging with photobleaching," Proc. Natl. Acad. Sci. U.S.A. **101**, 6462–6465 (2004).
14. M. Nirmal, B.O. Dabbausi, M.G. Bawendi, J.J. Macklin, J.K. Trautman, T.D. Harris, and L.E. Brus. "Fluoroscence intermittency in single cadmium selenide nanocrystals," Nature **383**, 802–805 (1996).
15. S. Hohng and T. Ha. "Near-complete suppression of quantum dot blinking in ambient conditions," J. Am. Chem. Soc. **126**, 1324–1325 (2004).
16. M. Funaro, E. Oja, and H. Valpula. "Independent component analysis for artefact separation in astrophysical images," Neural Networks **16**, 469–478 (2003).
17. J.-F. Cardoso. "Blind signal separation: statistical principles," Proc. IEEE **86**, 2009–2025 (1998).
18. A. Hyvärinen. "Fast and robust fixed-point algorithms for independent component analysis," IEEE Trans. Neural Networks **10**, 626–634 (1999).
19. J. Hurri, H. Gävert, J. Särelä, and A. Hyvärinen. FastICA: "An implementation of the fast fixed-point algorithm for independent component analysis in MATLAB, version 2.3, 2004," Helsinki University of Technology, `http://www.cis.hut.fi/projects/ica/fastica/`.
20. B. Richards and E. Wolf. "Electromagnetic diffraction in optical systems. II. structure of the image field in an aplanatic system," Proc. R. Soc. London A **253**, 358–379 (1959).
21. T.Q. Pham, M. Bezuijen, L.J. van Vliet, K. Schutte, and C.L. Luengo Hendriks. "Performance of optimal registration estimators," Proc. SPIE **5817**, 133–144 (2005).
22. R. Ando, H. Mizuno, and A. Miyawaki "Regulated Fast Nucleocytoplasmic Shuttling Observed by Reversible Protein Highlighting," Science **306**, 1370-1373 (2004).

1. Introduction

In fluorescence microscopy, the use of quantum dots (QDs) in biological imaging applications offers many advantages over traditional chemical fluorophores and visible fluorescent proteins, including photostability; narrow but tunable emission spectra [1]; and a broad spectral excitation cross-section. The recent availability of functionalized QDs has initiated their use in imaging studies of many biological systems [2, 3] and this trend will undoubtedly continue.

The best lateral resolution of a typical confocal microscope is on the order of 200 nm. Techniques for improving resolution to resolve fluorescence emitters with distance separations from 10-100 nm such as I^5M [4], 4Pi [5], STED [6, 7], and Saturated Patterned Excitation [8] tend to be complicated and expensive. In addition, many experiments do not require high resolution *per se*, but rather the ability to identify and precisely localize single fluorescent particles at the nanometer scale [9, 10]. However, the images of closely associated particles usually overlap. Separation in such cases has been achieved by use of multiple fluorophores of differing emission wavelength [11], fluorescence lifetime determinations [12], and photobleaching [13]. Unfortunately, techniques that require particles with different spectral properties suffer from chromatic aberrations and/or variations in the micro-environment, and separation by successive photobleaching limits the range of dynamic observation.

Here we exploit the fluorescence intermittency or 'blinking' of individual fluorophores to separate the emission of single fluctuating sources from within a group of like sources. If these blinking processes can be assumed to be statistically independent for each emitter, information about each individual fluorophore is encoded in the form of its temporal intensity fluctuations. Here we report the performance of a separation technique based on Independent Component Analysis (ICA) in the context of two-point resolution, that is, the ability to accurately localize

#7770 - $15.00 USD Received 10 June 2005; revised 14 August 2005; accepted 26 August 2005

two point emitters as a function of their separation.

Quantum dots are noted for random intermittency in their photoluminescence intensity [14, 15] and are particularly suited for this investigation. Under conditions easily obtainable with a standard wide field fluorescence microscope, i.e. a $60\times$ 1.4 numerical aperture (NA) objective, and a 100 W HBO lamp with a 435 nm$\pm$20 nm bandpass excitation filter, the blinking of individual QDs can be observed by eye or imaged with a sensitive CCD camera, and provides sufficient intensity and modulation for successful image processing.

Independent Component Analysis is a technique that has been applied to a broad spectrum of problems including the removal of artefacts from astronomical images [16] and image processing [17]. ICA is based on the central limit theorem, which states that a sum of statistically independent non-Gaussian variables (sources) tends to be described more closely by a Gaussian distribution than each individual source distribution. The ICA technique maximizes a measure of non-Gaussianity when unmixing sources from the detected signals. In the context of the work presented here, the unmixed sources represent the temporal intensity fluctuations of individual blinking emitters.

One measure of the non-Gaussianity of a variable y is the negentropy J, defined by $J(y) = H(y_{gauss}) - H(y)$. $H(y)$ is the differential entropy $H(y) = -\int f(y) ln f(y) dy$ [18], where $f(y)$ is the probability distribution function of y and y_{gauss} is a random Gaussian variable with the same variance as y. Negentropy has the property that it is always non-negative and is only zero if y has a Gaussian distribution. For calculational efficency, the FastICA algorithm [18, 19] used in this study uses an approximation of negentropy given by $J(y) \propto [E\{G(y)\} - E\{G(v)\}]^2$ where v is a Gaussian variable with unit variance and zero mean, E signifies the expected value and in the investigation described here $G(u) = log(cosh(u))$ although other choices are possible.

The applicability of ICA requires that the following conditions be met:

- The individual fluctuations of the sources to be resolved must be statistically independent. The blinking of QDs is a stochastic process and is thought to be influenced by surface defects that are unique to individual QDs [15]. Thus temporal fluctuations of individual QDs can be considered independent.

- The probability distributions must be non-Gaussian. The time scale of blinking QDs can be as long as seconds. Thus, sampling at shorter time scales will shift the temporal intensity distribution from a Gaussian towards a bimodal distribution as more complete "on" or "off" events are measured.

- The mixing of the sources to the detectors is linear and the mixing coefficients are not identical. Here, the detectors are the individual pixels of the CCD camera and we assume the light from each QD adds linearly in each pixel as expected for mutually incoherent emitters. If the mixing coefficients are identical, the emitters are located at identical positions and cannot be separated.

- The number of detectors is equal to or greater than the number of sources. This condition specifies that the maximal limit to the number of separable sources in a given area is equal to the number of pixels (N) detecting light from the emitting sources. In this context, it is worth noting that oversampling the image may increase the number of potentially separable sources.

We make use of the ICA principle in the following way: A time series of images is written as a $N \times T$ data matrix $\mathbf{x}$ where T is the number of temporal images and N is the number of pixels. Each row of $\mathbf{x}$ represents the time series of a pixel. In the ICA model the data matrix can be written as $\mathbf{x} = \mathbf{As}$ where $\mathbf{s}$ is a $n \times T$ source matrix where n is the number of sources, and $\mathbf{A}$ is a $N \times n$ mixing matrix. In the noise-free case, the rows of $\mathbf{s}$ contain the temporal fluctuations for

#7770 - $15.00 USD Received 10 June 2005; revised 14 August 2005; accepted 26 August 2005

each individual emitter and the columns of **A** contain the strength of the signal in each pixel. In the context of this paper, the goal is to compute **A**, which contains the spatial information about each emitter. To achieve this the problem can be restated as $\mathbf{s} = \mathbf{W}\mathbf{x}$ where **W** is $n \times N$ weighting matrix. ICA is applied to find **W** and thus **s**, the rows of which contain the signals from independent emitters. ICA uses the property that independent sources **s** should have the least Gaussian intensity distribution. We employ the symmetric approach that maximizes the quantity $J_{total} = \sum_i^n J(\mathbf{s}_i)$, where $\mathbf{s}_i$ is the ith row of **s** and J is the approximation of the negentropy as described above.

To carry out the ICA decomposition, we use the MATLAB (The MathWorks, Inc.) implementation of the FastICA algorithm [18, 19]. The data matrix **x** is submitted to the FastICA routine, which is instructed to extract two components. In brief, the FastICA algorithm performs the following operations:

1. Centers the data by subtracting the mean of each row in **x**. The ICA model only utilizes relative pixel-to-pixel temporal fluctuations in the decomposition.

2. Projects the centered data onto a specified number of principle component directions found in a principle component analysis of the covariance matrix of the centered data. This is followed by normalizing the variances along these directions to unity (whitening). A data reduction operation for noise removal can be incorporated by projecting the data matrix onto a limited number, n, of principle component directions. These two processes can be written as a multiplication by an $n \times N$ matrix **K**. The variances are normalized because calculation of the non-Gaussianity is measured by comparison to a Gaussian variable with zero mean and unit variance.

3. Iteratively determines an $n \times n$ matrix **B**, where $\mathbf{s} = \mathbf{B}^{\mathbf{T}}\mathbf{K}\mathbf{x}$ by maximizing the non-Gaussianity in the rows of **s**; **B** is constrained to be orthonormal.

4. Returns **s**, **A** and **W** where $\mathbf{A} = \mathbf{K}^{+}\mathbf{B}$ ($^{+}$ indicates pseudo-inverse) and $\mathbf{W} = \mathbf{B}^{\mathbf{T}}\mathbf{K}$.

The n rows of the estimated mixing matrix, **A**, now contain the strength of the source for each pixel. Rearranging the pixels in reverse manner as they were arranged into the columns of **x** yields the images of each independent emitter.

2. Simulations

We investigated the ability of the ICA to locate two QDs as a function of their separation and noise level. The simulation was constructed as follows. Each dot was represented by the point spread function (PSF) of a point emitter calculated for an ideal 60× 1.45 NA objective [20] using random polarization and vector theory (aplanar apodization). The PSF image was normalized so that the sum of all pixels equaled a target expected total photon count and was centered about a given position with sub-pixel resolution by shifting using multiplication with an exponential phase function in the Fourier-domain. Here the term 'expected' takes its statistical meaning, i.e. the mean measured value. Pixel sizes of 6.45 μm in the image plane were simulated to represent the Hamamatsu Orca-AG camera used in the experiments. The image of the PSF on the camera was replicated 500 times, representing a time series of 500 images acquired with the camera. Each image of each dot was then multiplied by a random number selected from a uniform distribution between 0 and 1 to simulate the blinking behavior of the dot. We did not attempt to approximate the true blinking behavior of QDs, but rather simulated their non-Gaussian behavior. Finally, the images of the two dots were combined and Poisson noise applied to each pixel of every image based on the expected pixel photon count.

#7770 - $15.00 USD Received 10 June 2005; revised 14 August 2005; accepted 26 August 2005

The data stack was rearranged to yield a matrix with each row being the time sequence of an individual pixel. This matrix was submitted to the FastICA algorithm as described in the previous section. The returned mixing matrix **A** was rearranged into images, each of which should ideally contain the individual image of each QD. The simulation was repeated 50× for each combination of spot separation (0.01 to 2 pixels) and maximal expected photon count (100 to 10000 photons). Due to the extreme photostability of QDs, acquisition of photon numbers in this range is experimentally realistic. The position of the point emitter in each of the two images returned from the ICA analysis was found using a maximum likelihood estimation (MLE).

When fitting data to a model in a process with Poisson distributed values the best fit (MLE) comprises minimizing the I-divergence, which is given by $Idiv(data, model) = \frac{1}{N}\sum_{i=1}^{N}[data_i \log\left(\frac{data_i}{model_i}\right) - (data_i - model_i)]$, where N is the number of pixels in the measured ($data_i$) and modeled ($model_i$) images. The parameters to optimize that generate the model image in the case of a single emitter are the *x*, *y* position of a generated PSF image and its intensity. The MLE analysis of the sum image, which gives the conventional state of the art results when no blinking statistics are used but the total number of collected photons is kept equal, is performed with an estimation assuming two point emitters.

To compare the performance of the ICA/single emitter analysis to the MLE fit of the sum image, the mean of the relative localization error over the 50 simulations with identical parameters was computed. The relative localization error (the localization error divided by the separation), is given by $\frac{\left|\mathbf{P}_{known,dot1}-\mathbf{P}_{found,dot1}\right|+\left|\mathbf{P}_{known,dot2}-\mathbf{P}_{found,dot2}\right|}{2\left|\mathbf{P}_{known,dot1}-\mathbf{P}_{known,dot2}\right|}$ where $\mathbf{P}$ is the position vector (x,y) of the emitter. Fit positions with errors greater than 4 pixels, which primarily effects the MLE fit of the sum image by increasing the mean relative error, were not used in calculations of the mean relative error. At these large separations, the results could be readily rejected by inspection of the images and thus would not affect the interpretation of an unknown sample. The results showing the mean relative separation error for the two methods under varying separation and expected photon count are shown in Fig. 1(a). In Fig. 1(b) the effect of smoothing the data set and PSF in *x* and *y* before analysis using an isotropic Gaussian kernel with varying σ is demonstrated. Smoothing with a Gaussian kernel has the effect of trading spatial resolution for increased signal-to-noise. As can be seen in Fig. 1(a), localization accuracy was strongly dependent on signal-to-noise and Fig. 1(b) shows a beneficial tradeoff for the localization accuracy at a Gaussian kernel size of σ = 1 pixel.

The simulations show that single particle localization in the images found by ICA analysis yielded a significant improvement in the localization accuracy compared to fitting the MLE with a two spot parametric model. In the case of 10^4 maximal expected number of photons per frame, the ICA approach yielded excellent localization accuracy of < 0.2 pixels, which corresponds to $< \lambda/30$.

3. Experimental Results on Quantum Dots

We experimentally demonstrated the ability of the ICA analysis to resolve closely spaced QDs with a randomly distributed sample of QDs on a coverslip. The density was sufficient to produce groups of dots with separations smaller than the optically resolvable separation of the microscope.

3.1. Materials and Methods

A 1 nM solution of QDs is made by dilution of an original stock of 1 μM Qdot 655 Streptavidin Conjugate QDs (Quantum Dot Corp., Hayward, CA, USA) with the incubation buffer provided with the QDs. One well of an eight well microscope slide was filled with 300 μL of 50 mM NaCl. We have determined that NaCl $\geq$ 50 mM induces adherence of QDs to uncoated cover-

#7770 - $15.00 USD Received 10 June 2005; revised 14 August 2005; accepted 26 August 2005

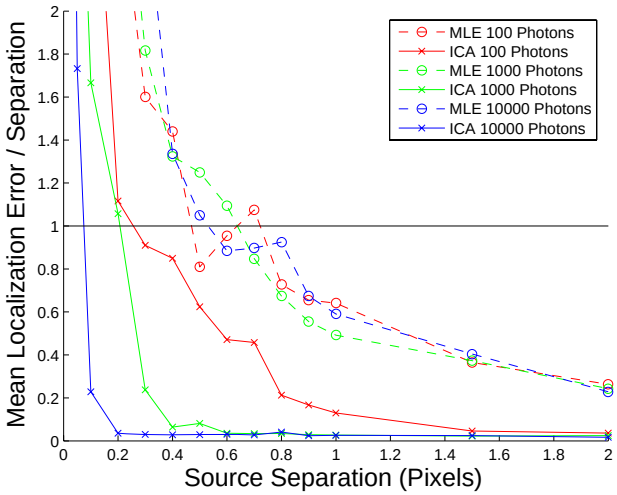

(a)

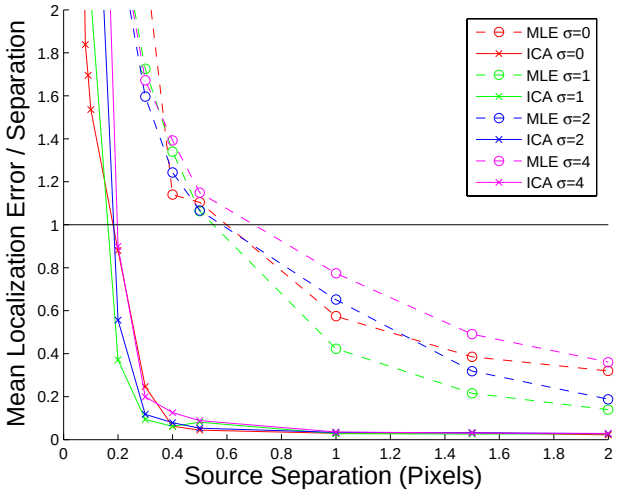

(b)

Fig. 1. Ability of the ICA approach to localize two blinking sources compared to fitting the sum image to a 2 source model with a maximum likelihood estimate. Each point represents the average of 50 simulations. To account for outliers (found only in the MLE analysis), localization errors > 4 pixels were ignored. The photon counts refer to the expected maximum photons per dot per image. Each pixel corresponded to 108 nm as given by the geometry of the experiments. The black line indicates where the localization error was equal to the separation. (a) The mean localization error divided by separation (b) 1000 expected max photons as for one of the above cases but with the data series and the PSF smoothed (Gaussian kernel with indicated width σ) in x and y before analysis. A smoothing with σ = 1 pixel leads to a beneficial trade off between signal to noise and spatial resolution.

#7770 - $15.00 USD
Received 10 June 2005; revised 14 August 2005; accepted 26 August 2005

glass surfaces. 10 μL of 1 nM QDs were added to the well. After 10 min, a sufficient density of QDs adhered to the bottom of the well, which was then rinsed with 50 mM NaCl to remove any remaining free QDs.

Measurements were performed using an inverted Olympus IX71 microscope (Olympus Deutschland GmbH, Hamburg, Germany) with a 60$\times$ 1.45 NA oil objective. The filter set consisted of a 440/20 excitation filter, 505 nm DRLP dichroic mirror (Omega Optical, Brattleboro, VT, USA) and 655/40 quantum dot filter (Chroma Technology, Rockingham, VT, USA). The detector was a CCD camera (model Orca-AG with 6.45 micron pixels, Hamamatsu Photonics UK Ltd, Welwyn Garden City, UK). A series of 500 images of size 256$\times$256 pixels were taken with an exposure time of 10 ms, yielding a total exposure time of 5 s and, with the overhead due to camera readout, a total acquisition time of approximately 12 s. A second series of images with identical parameters was taken with no light incident on the camera. This background estimation was averaged over time, then subtracted from each image of the data series on a pixel by pixel basis in order to remove any pixel-dependent camera offset which could negatively affect image registration.

3.2. Analysis of Experimental Data

The ICA technique is particularly sensitive to lateral drift, or defocus during the acquisition of the time series data. Each frame of the times series was aligned to the mean of 10 images selected from the beginning of the time series using an algorithm [21] that achieves the theoretical limit for image registration. Using Eq. 10 of [21], which requires the calculation of the energies in the image gradients and the signal-to-noise ratio, for the data considered here the registration was calculated to be better than 1/20th of a pixel, corresponding to $\sim$ 5 nm. After registration, three smaller 32$\times$32 subsections were selected for analysis from the acquired time series. Each of these regions was smoothed with a Gaussian filter of σ = 1 pixel and processed identically as described above.

The results of the ICA procedure are shown in Fig. 2. The control in Fig. 2(a) represents a situation in which 2 QDs were separated by a distance larger than the resolution limit of the microscope. In this case, it is clear that the ICA procedure correctly returned the images of the individual quantum dots. Localizing each dot individually yielded a separation of 435 nm. The MLE localization determined a separation of 595 nm. The discrepancy between the MLE and ICA approach was not expected from the simulations, but may indicate that the exact form of the experimental PSF becomes more important in the MLE case. Fig. 2(b) shows a case in which it was not apparent that more than one QD was present. However, the ICA procedure found 2 components appearing to be QDs and the localization of each QD yielded a separation of 23 nm. To estimate the localization error, a comparison was made between the experimental conditions and the simulations. The known gain of the camera was used to estimate the measured photons per frame per QD. The value of $\sim$ 500 photons corresponds to a maximal value of $\sim$ 1000 photons, which was the quantity investigated in the simulations. The data was smoothed with a Gaussian kernel of σ = 1 pixel before analysis yielding conditions similar to the curves in Fig. 1(b), and indicating the error in particle localization was approximately 20 nm. Given the determined particle separation and localization error, the separation is consistent with the two dots having formed a dimer before adhering to the coverslip. In Fig. 2(c), only one component representing a QD was found, the other being noise.

4. Discussion and Conclusions

Simulations investigating the localization error as a function of the distance between two point emitters show that an analysis using Independent Component Analysis to first separate emitters via their temporal fluctuations followed by single particle localization performs better than a

#7770 - $15.00 USD Received 10 June 2005; revised 14 August 2005; accepted 26 August 2005

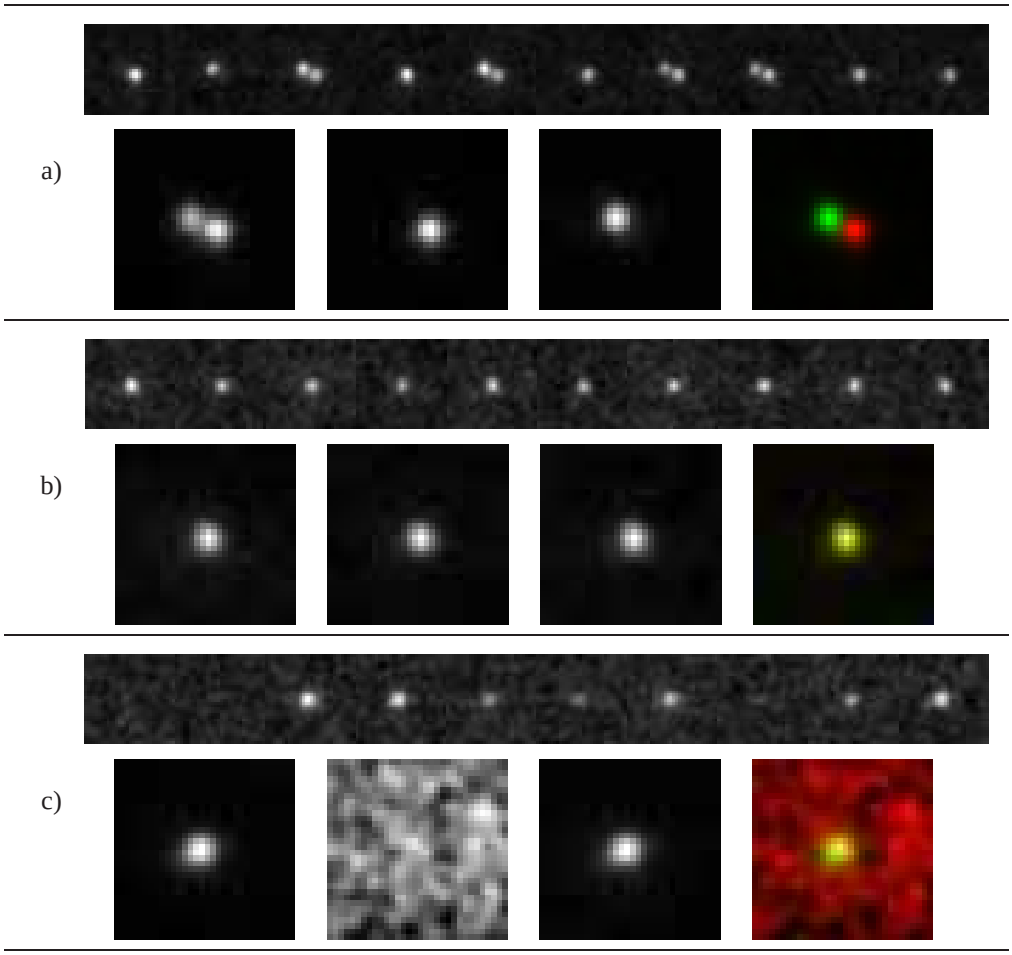

Fig. 2. The results of the ICA decomposition for three examples of experimentally acquired blinking QD data sets. Top: 10 frames from the time series. Bottom, left to right: Sum image of time series, ICA returned component 1, ICA returned component 2, color overlay of component 1 and 2. Images are 32×32 pixels with pixel size of 108 nm. (a) Two widely separated blinking quantum dots, separation distance is found to be 435 nm. (b) Two closely spaced QDs, separation is found to be 23 nm. (c) Only a single quantum dot is found, the other component is noise.

traditional analysis based on fitting the sum image to a two-spot parametric model. The technique was demonstrated with experimental data and functioned within the limits established by the simulation based on 655 nm emission QDs deposited on coverslips.

The simulated and experimental data presented here were two-dimensional. However, the method can be extended to three dimensions in a straightforward manner. If only a two-dimensional slice is imaged, the method of separation should still work on particles that are out of focus and some three dimensional position information can be obtained from the analysis of their individual images. A combination of stereo microscopy methods with the blinking localization scheme could enhance the three-dimensional performance, as would the acquisition and analysis of serial sections.

#7770 - $15.00 USD Received 10 June 2005; revised 14 August 2005; accepted 26 August 2005

Simulations show that the localization accuracy is dependent on the correct predetermination of the number of emitters as an input to the FastICA decomposition. The practical use of this analysis would benefit from development of a robust method for determining the number of localized emitters. In our experience, it is not possible to determine the number of QDs in a cluster solely by analysis of the intensity. However, it is possible that improvements in the synthesis of QDs will lead to a greater uniformity such that simple intensity based determinations will be feasible. For currently available QDs, a robust method for determination of cluster sizes should utilize all available information, including the mean intensity, maximum intensity, relative strength of the eigenvalues found from the Principle Component Analysis of the pixel-to-pixel covariance matrix, and the temporal course of the measured intensity. The successful classification of images returned from ICA approach as point emitters could also be used. An additional method would be to label the QDs with a fluorescent dye that emits at a wavelength other than in the QD band, and use these data for intensity based determinations.

Although only two emitters were considered in detail, we demonstrated the robustness and limits of the ICA method by simulating 3 blinking emitters positioned within a 100 nm diameter. The simulation consisted of 500 time frames, in which the expected maximal photons per QD per image was 1000. No smoothing was performed. The images found using the ICA method assuming 2,3 or 4 emitters and the localization of the emitters are shown in Fig. 3. Panels (a) and (b) demonstrate that underestimating the number of emitters can lead to incorrect localization values, whereas overestimating the number of emitters may lead to spurious images that somewhat resemble point emitters (Fig. 3(h)). We have found that spurious PSF like images become more common as the number of emitters within a region increases. It also becomes difficult to reliably separate more than 5 emitters within a 200 nm diameter area, but this should be taken as a limitation of the present approach and not of the blinking-based separation procedure in general.

The performance of the technique could be further improved inasmuch as the current ICA scheme does not make use of any of the following *a priori* information: spatial relationship between the pixels, shape of the PSF, the photon Poisson distribution, the positivity of fluorescence emission, or the temporal intensity distribution of QDs, the temporal order of the images. The described ICA scheme could possibly be modified to account for the above information. However, other attractive schemes could also be based on pixel-to-pixel cross-correlation. In addition, the use of a full Maximum Likelihood based noise model, including the blinking kinetics and image formation appears very attractive. Such methods may enable a reliable, rapid and fully automatic localization of thousands of QDs in a single sequence of images. Thus, structures in cells could be stained with a moderate concentration of QDs, which then after individual localization, would reconstitute structures of interest (e.g. the cytoskeleton) by essentially painting them in a ”pointillistic” fashion.

A current and general limitation of the method is the requirement of particle positions to remain stable over the time course of the experiment. However, a general drift of the whole field is not a problem and can be accounted for as described [21]. One should also be able to compensate for relative displacements of clusters of particles as long as they can be resolved or separated and no movement occurs within the clusters. In the application of the method to biology, thermal (Brownian) fluctuations may pose a fundamental limit to the attainable resolution, which can then only be improved by better methods of immobilization such as by multivalent binding.

The application of the blinking analysis to fluorescence emitters undergoing triplet state blinking would require an array detector with the ability to sample at rates higher that the blinking kinetics and detecting a sufficient number of photons per frame. In general, a high intensity excitation may be required. Although current CCD cameras are unable to sample in the

#7770 - $15.00 USD Received 10 June 2005; revised 14 August 2005; accepted 26 August 2005

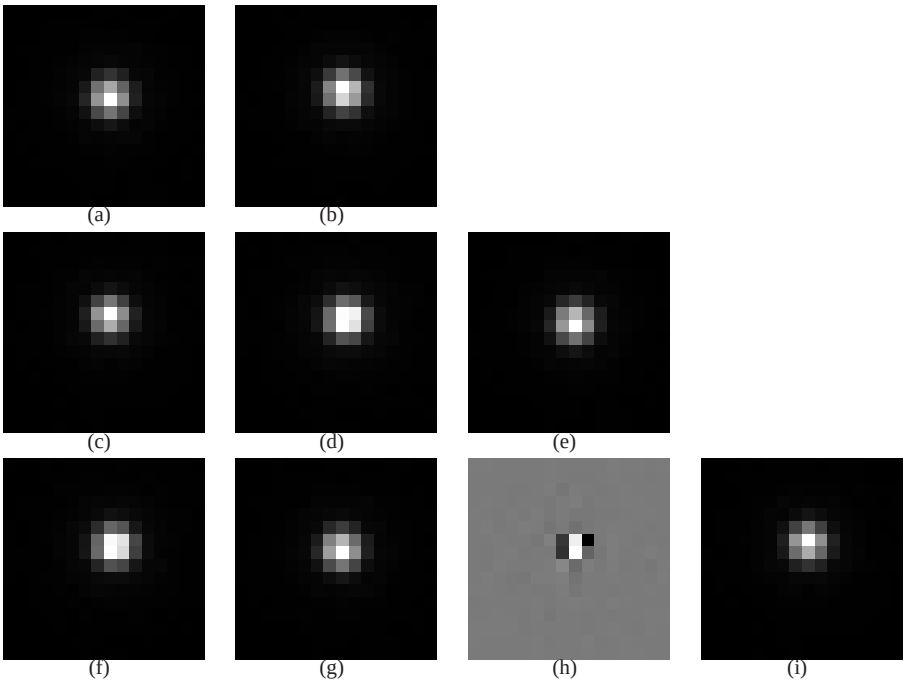

Fig. 3. The results of the ICA decomposition of 3 blinking emitters. The coordinates in pixels with respect to the center of the image are (0.9501,-0.2311), (1.3380,-0.5467) and (0.9881,-0.7297). The data series was simulated with 1000 photons per dot per QD and 500 time frames. Images are 16×16 pixels with a pixel size of 108 nm. (a and b) are the images found when the ICA analysis assumes 2 emitters. Localization yields coordinates of (0.9801,-0.2139) and (1.1497,-0.6448). (c, d, and e) are the images found when the ICA analysis assumes 3 emitters. Localization yields coordinates (1.0024,-0.7596),(1.3447,-0.5623) and (0.9553,-0.2648). (d, e, f and g) are the images found when the ICA analysis assumes 4 emitters. Localization yields coordinates of (1.3397 -0.5558),(0.9487 -0.2636),(0.0485 0.2060), and (0.9897 -0.7659).

μs domain, other approaches can be envisioned. A small array of high speed detectors such as avalanche photodiodes or multianode photomultiplier tubes could be used to serially investigate small regions of a sample. A pump-probe approach of illumination and image acquisition could also lead to the desired statistics in the images even with comparatively slow data readout. Advances in electron multiplying CCD cameras and other detectors may also yield high sensitivity, very high speed array detectors. Furthermore, we note that photobleaching can be considered an on-off event similar to blinking that would generate contrast useful for separation (as used in [13]) and is not necessarily detrimental to imaging except in the case of repeated measurements. The reversible photo-conversion techniques based on photochromism offer additional possibilities [22].

Combinations of discrimination by blinking individuality with and by color or other schemes should increase the maximal concentration of particles that can be separated into individual components. A similar effect can be expected from a combination of resolution enhancing schemes leading to greater localization precision, since they decrease the spatial extent of the PSF.

#7770 - $15.00 USD Received 10 June 2005; revised 14 August 2005; accepted 26 August 2005

Acknowledgments

We thank Peter Verveer for providing routines for PSF calculation. Stephan Schäfer is thanked for his help with experiments. We thank Dmitry Cherny for his efforts in characterizing QDs using electron microscopy. Bernd Rieger was supported by a TALENT fellowship from the Netherlands Organization for Scientific Research (NWO).

#7770 - $15.00 USD Received 10 June 2005; revised 14 August 2005; accepted 26 August 2005